

North–South anisotropy in the arrival directions of the extremely high energy cosmic rays

D. S. Gorbunov, S. V. Troitsky¹⁾

*Institute for Nuclear Research of the Russian Academy of Sciences,
60th October Anniversary Prospect 7a, 117312, Moscow, Russia*

Submitted June 6, 2003

We study the large-scale distribution of the arrival directions of the highest energy cosmic rays observed by various experiments. Despite clearly insufficient statistics, we find a deficit of cosmic rays at energies higher than 10^{20} eV from the Northern part of the sky. We speculate on possible explanations of this feature.

PACS: 98.70.Sa

1. The physics of the highest energy cosmic rays continues to attract significant interest of both particle physicists and astrophysicists. Experimental data allow to determine energies and arrival directions of the cosmic particles and may give some hints about their nature. At energies of order 10^{19} eV, spectra measured by different experiments are in a good agreement modulo overall normalization. Contrary, two major experiments disagree about the observed flux and shape of the spectrum at highest energies, $E \gtrsim 10^{20}$ eV: the data from the HiRes experiment exhibit the suppression of the flux, the so-called GZK feature [1, 2], while the AGASA experiment does not see the suppression. Arrival directions of the cosmic rays with energies $E \gtrsim 10^{19}$ eV are distributed isotropically over the sky (see, for instance, Ref. [3]) and clustered at small angles [3, 4, 5]. In this note, we focus on the highest energy region, $E \gtrsim 10^{20}$ eV, and demonstrate that the current data exhibit a trend to non-uniform distribution of the arrival directions. Namely, there is a deficit of events from a large region around the celestial North pole.

For the most energetic cosmic rays observed by AGASA, the absence of particles coming from the North has been pointed out in Refs. [6, 7, 8]. However, the distribution of the arrival directions of these AGASA events is consistent with isotropy [9], given the non-uniform exposure. To test the conjecture of anisotropy (and also to improve statistics, still very poor), we include results from all Northern hemisphere experiments in our analysis. We do observe a non-uniform distribution of events with probability of this anisotropy to occur as a result of chance fluctuation about 1%; this would correspond to ~ 2.6 standard deviations for Gaussian distribution. If confirmed by better statistics, this observation might mean that at highest energies,

a new component appears in the cosmic ray flux. Indeed, it is widely believed now that at $4 \cdot 10^{19}$ eV $\lesssim E \lesssim 10^{20}$ eV, the dominant part of the cosmic rays are protons [10, 11] from active galactic nuclei (with BL Lac type objects being the most promising source candidates [12, 13, 14]). Due to the GZK effect, this component cannot explain even the most conservative HiRes flux at $E \gtrsim 10^{20}$ eV (see Refs. [15, 16] for a quantitative analysis). We will see that indeed, the anisotropy becomes significant at energies $E \gtrsim 10^{20}$ eV.

In the rest of the Letter, we discuss in detail the datasets used in this analysis, with special attention to the overall normalization of energies and to exposures of different experiments. We analyze the declination distribution of the highest energy events detected by all Northern hemisphere experiments, present the results of the Monte Carlo simulations to estimate the chance probability of the observed anisotropy, and study at what energies the anisotropic component becomes significant. We discuss possible ways to explain the effect and demonstrate its irrelevance to the AGASA/HiRes discrepancy. We emphasize that the number of events is too small to make a definite conclusion about the anisotropy and briefly discuss prospects for larger statistics.

2. Our basic data set (hereafter, Set I) consists of the cosmic rays with energies higher than 10^{20} eV observed by all experiments in the Northern hemisphere. Alternatively, we consider a set of cosmic rays with $E \gtrsim 4 \cdot 10^{19}$ eV observed by Volcano Ranch, Yakutsk and AGASA (Set II)²⁾. The latter set is useful in determination of the "critical" energy at which the new, anisotropically distributed, component becomes important. As it will be demonstrated below, this analysis points to $E \approx 10^{20}$ eV as the critical energy. Together

²⁾Arrival directions of events with $E < 10^{20}$ eV are unpublished for other Northern-hemisphere experiments.

¹⁾e-mail: st@ms2.inr.ac.ru

Experiment	J	η	B	A
(1)	(2)	(3)	(4)	(5)
Volcano Ranch	3.68 [17]	0.76	32	0.3 [18]
Haverah Park	2.22 [18]	0.90	54	0.9 [18]
Yakutsk	3.31 [18]	0.78	62	2.4 [18]
Fly's Eye	2.23 [18]	0.90	40	2.6 [18]
AGASA, $>10^{20}$ eV		0.86	36	4.6 [19]
AGASA, $<10^{20}$ eV	2.51 [18]	0.86	36	4.0 [3]
HiRes I mono	1.6 [20]	1.00	40	7.4 [20]
HiRes II mono	1.6 [21]	1.00	40	0.7 [21]

Table 1. Cosmic ray experiments. (1): name; (2): flux measured at 10^{19} eV (in units of $10^{-33} \text{ m}^{-2} \text{ s}^{-1} \text{ sr}^{-1} \text{ eV}^{-1}$) and reference; (3): energy normalization factor; (4): geographic latitude (in degrees); (5): total exposure (in units of $10^{16} \text{ m}^2 \text{ s} \text{ sr}$) (for the cosmic rays with energies above 10^{19} eV; for AGASA different exposures for published data above 10^{19} eV and 10^{20} eV; for Fly's Eye and HiRes – at 10^{20} eV) and reference.

with availability of data from fluorescent detectors at $E \gtrsim 10^{20}$ eV only, this determines the choice of the Set I.

When comparing data from different experiments, one should be careful about energy normalization. It is widely believed that at $E \sim 10^{19}$ eV, where the shapes of the spectra measured by different experiments agree quite well, the difference in overall normalization is due to systematic errors in the energy determination. For our purposes, it is sufficient to introduce correcting factors in energy values in such a way that the total flux measured at $E = 10^{19}$ eV by different experiments would coincide with the flux measured by a given (no matter which one) reference detector (HiRes in our case)³⁾. The study of the dependence on the choice of the reference detector is completely equivalent to the study of the dependence on the "critical" energy performed below.

It follows from the definition of the flux that the corrected energy $E' = \eta E$, where E is the reported energy of an event and $\eta = (J_{\text{ref}}/J)^{1/3}$. Here, J_{ref} and J are the cosmic ray fluxes measured by the reference detector and the detector under consideration, respectively. The fluxes J at $E \sim 10^{19}$ eV and normalization factors η are listed in Table 1 together with information required to calculate and compare exposures of the experiments and with references.

For the data sample, we took the most recent publicly available data: we impose zenith angle cuts of 60°

³⁾We normalize all fluxes to HiRes data because otherwise the HiRes dataset is not complete.

for all experiments except AGASA and Haverah Park for which 45° cut is adopted.

Three experiments (Haverah Park, Yakutsk and HiRes in the monocular mode) have considerable exposure at the ultra-high energies but contributed no events to the Set I (though their exposure was taken into account).

Energies of the Haverah Park events published in the Catalog [22] were reconsidered twice, in Refs. [23] and [24]. According to the most recent publication [24], the energy of the highest event is $E \approx 8.3 \cdot 10^{19}$ eV. Revised event-by-event data were not published.

The Yakutsk event with the energy $E \approx 1.2 \cdot 10^{20}$ eV has $E' \approx 9.4 \cdot 10^{19}$ eV thus it is not included in Set I (note that its declination [25] is $\delta \approx 45^\circ$, so it would only support our conclusions).

Coordinates of the Volcano Ranch events, both of the only shower with $E > 10^{20}$ eV and of showers with lower energies (Set II) were taken from Ref. [22].

For the Set I, we use the most recent AGASA data from the experiment's web page [9]. From eleven events, eight are left after rescaling from E to E' . The lower energy data for the Set II are available for a shorter period of operation, Ref. [3]. This is the reason for smaller exposure used for the lower-energy data, as indicated in Table 1.

For fluorescent detectors, the data are published for the highest energy events only. The single Fly's Eye event contributing to Set I is described in detail in Ref. [26]. For the HiRes I detector in the monocular mode, we take the working period reported in Ref. [20] (v.2). The arrival direction of the single event with $E > 10^{20}$ eV registered during that period and passed all cuts is taken from Ref. [27]⁴⁾.

3. Different parts of the sky are seen by various experiments with different exposures. For ground arrays, we use the geometrical differential exposure. A small plaquette of area $d\sigma$ [sr] on the celestial sphere at the zenith angle θ is effectively seen by the area $dA = A_0 \cos \theta d\sigma$ of a ground array, where A_0 is the maximal aperture. The total exposure for a plaquette $d\sigma$ can be found by integration over the working time of the detector. The explicit formulae which result from this integration for a continuously operating ground array are given in Ref. [29]. The exposure does

⁴⁾Preliminary, the HiRes experiment reported two more events with $E > 10^{20}$ eV observed in the stereo mode. Their arrival directions, as well as the experiment's exposure, can be inferred from Ref. [28]. We addressed the HiRes collaboration for several times asking for a permission to use these data but received no answer. Inclusion of these two events would support our conjecture on anisotropy and would lower the Monte Carlo probability for the Set I from 0.9% down to 0.6%.

not depend on the right ascension α in this case. At energies 10^{19} eV $\lesssim E \lesssim 10^{20}$ eV, these expressions are in excellent agreement with the observed data (see Fig. 1(b))⁵⁾. To obtain the normalization factor A_0 , important for any analysis which involves data of different experiments, one has to integrate $dA/d\sigma$ over $d\sigma$ and to compare the resulting total exposure A with the published value listed in Table 1.

For the fluorescent detectors, this simple geometrical estimate does not work. Their exposure is affected by many factors and depends both on α and δ , in different ways at different energies (dependence on α arises due to non-continuous operation of these detectors: they work on clear moonless nights only). In particular, the α dependence of the exposure of the HiRes I detector was presented in Ref. [31]. For the δ dependence, we use the actual distribution of the observed events in declination obtained from the plots of arrival directions in Ref. [28] for energies $E > 10^{19}$ eV. Though one could expect different declination dependence of the exposure for higher energies, the one we use agrees quite well with the distribution of the HiRes I events with $E > 10^{19.5}$ eV, Ref. [32]. For the Fly’s Eye experiment, we use the declination distribution of events with $E > 3 \cdot 10^{19}$ eV from Ref. [33].

4. We are ready to analyze the global distribution of the arrival directions. To illustrate the anisotropy, we divided the observed part of the sky into five bands in declination with equal areas, and integrated the exposures over these bands. The exposures were compared then to the number of observed events, band per band. The results for the Set I of cosmic rays are shown in Fig. 1(a). The left (red) bar in each pair corresponds to the exposure per band, normalized to the total number of events in the sample. It represents the number of events expected for isotropy. The right (blue) bar corresponds to the actual number of observed events in the sample. The deficit of events in the Northern bin is clearly seen.

To estimate this effect quantitatively, we perform Monte Carlo simulations of the arrival directions of cosmic rays. We determine the exposure function

$$a(\delta) = N \sum_i \frac{dA_i}{d\delta},$$

where the sum is taken over all relevant experiments, each one’s total exposure reflected in A_{0i} , and N is the constant such that $\max_{\delta} a(\delta) = 1$. The code generates

⁵⁾It is probably the $\cos \delta$ factor in $d\sigma = \cos \delta d\delta d\alpha$ which lead to the discrepancy of the exposures from Ref. [29] with the observed distributions of arrival directions in δ claimed in Ref. [30].

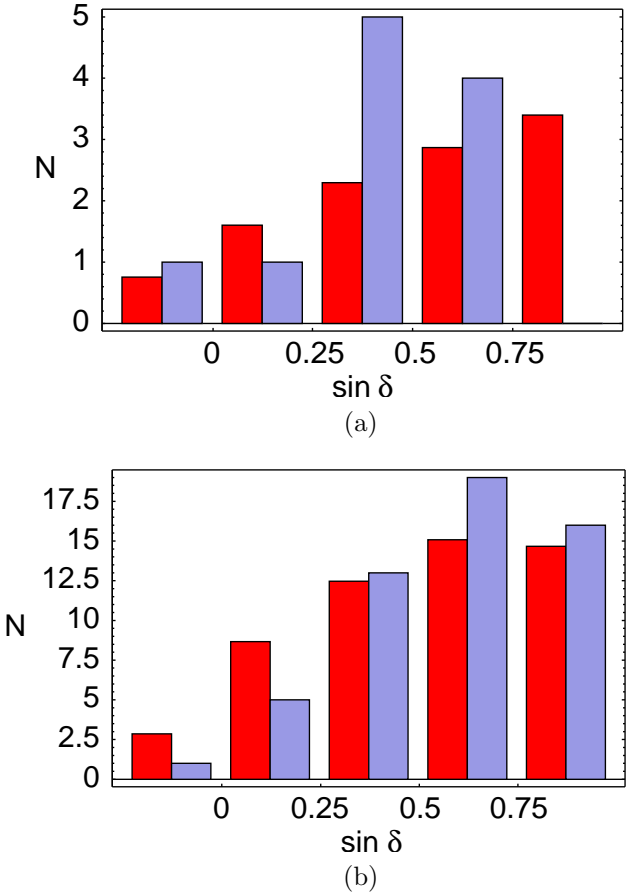


Fig. 1. Expected and observed distributions of declinations of the cosmic rays (a) from the Set I ($E' > 10^{20}$ eV); (b) from the Set II ($4 \cdot 10^{19}$ eV $< E' < 10^{20}$ eV).

a value of declination δ in such a way that the resulting cosmic rays cover the sky uniformly; then it either accepts (with the probability $a(\delta)$) or rejects this event and proceeds to the next one until the total number of accepted events reaches the number of events in the real dataset. In this way, a sufficient number of mock sets is produced. The number of sets with no events in the Northern bin, divided by the total number of sets, determines the probability to observe the anisotropy by chance. For the basic dataset and the Northern bin determined above, the corresponding probability is about 1%.

To study the stability of our results, we calculated the probabilities to observe the actual number of events in the Northern bin, $\delta > \delta_0$, for different values of δ_0 (see Fig. 2). The position of the broad minimum determines the size of the Northern “zone of avoidance”.

Let us study now the question at which energy the anisotropically distributed component becomes impor-

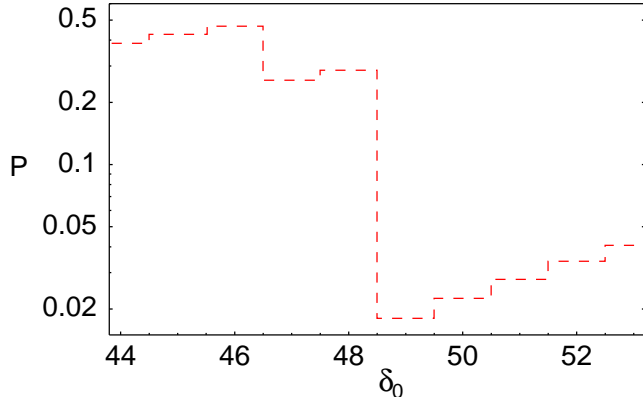


Fig. 2. Probability to observe the actual number of events in the Northern bin ($\delta > \delta_0$) as a result of a statistical fluctuation, versus δ_0 (Set I, $E' > 10^{20}$ eV).

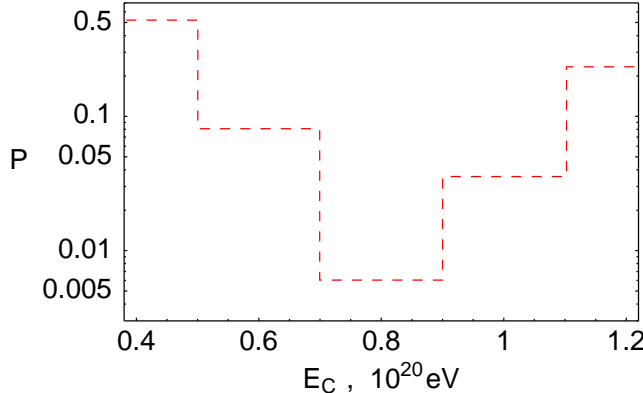


Fig. 3. Probability to observe the actual distribution of events as a result of a statistical fluctuation versus the critical energy E_c : included in the sets are data from Set II with $E' > E_c$.

tant. We use the Set II for this purpose. In Fig. 3, based on subsets of the Set II, we present the probability of the actual number of events to occur in the Northern bin as a result of a random fluctuation of the isotropic distribution for different lower energies of the cosmic rays in the set. The result is consistent with expectations: at lower energies, we confirm the well-known statement about isotropic distribution; at higher energies, $E > 10^{20}$ eV, protons from active galactic nuclei are no longer dominant in the cosmic ray flux because of the GZK effect, and the new component is responsible for the observed events, distributed anisotropically.

Several comments are in order. First, the chance probabilities at $E' > E_c = 10^{20}$ eV presented in Fig. 2 (Northern bin corresponds to $\delta_0 \approx 48.6^\circ$) and in Fig. 3 are of the same order, but do not coincide exactly. The reason is that the sets of experimental data (Set I and Set II) used in the analysis are different.

Second, because of experimental uncertainties in the determination of the energies and arrival directions of the cosmic rays, it is not well-grounded to consider lowest values of probability P plotted in Figs. 2 and 3 as exact numbers: some averaging over the uncertainty intervals in δ and E_c should be performed to get more reliable numbers. The resulting probabilities will be higher, but definitely the isotropy is excluded at the level of better than 2σ for Gaussian distribution.

Third, the lowest probability in Fig. 3 corresponds to critical energy $E_c \simeq 0.8 \cdot 10^{20}$ eV. With available data it is impossible to conclude whether this is the exact energy scale where the anisotropic component of ultra-high-energy cosmic rays becomes dominant. Indeed, apart from experimental uncertainties in energy determination, a systematic error is caused by an arbitrary choice of the reference detector necessary for a joint analysis of the data from different experiments (for instance, normalization to one of the ground arrays instead of HiRes would shift the minimum in Fig. 3 to $\sim 10^{20}$ eV).

5. Clearly, the number of events in our sample is insufficient to make a definite conclusion about anisotropy of the arrival directions. However, the current dataset gives a strong hint that the deficit of events with energies higher than 10^{20} eV and coming from the region $\delta \gtrsim 50^\circ$ is significant. If confirmed by future experiments, this fact might suggest that a new component emerges in the cosmic ray flux at extreme energies. The physics which could result in the observed distribution of declinations will be discussed elsewhere; we just mention two possible ways of explanation. Firstly, the Northern region can coincide with the direction to some large-scale cosmic structure which affects propagation of the cosmic rays at very high energies or causes inhomogeneous distribution of their sources (at 10^{20} eV this effect is not smeared out by galactic magnetic fields). The second option is that the primaries of the cosmic rays with $E \gtrsim 10^{20}$ eV interact with the geomagnetic field and produce showers in different ways at high and low latitudes⁶⁾. While the latter possibility could be checked with the Southern site of the Pierre Auger observatory, large detectors in the Northern hemisphere (such as the Northern Auger site, the Telescope Array or the EAS-1000 experiment) or full-sky cosmic observatories (EUSO, OWL, TUS) would be required to confirm or reject the first option.

The use of currently unpublished data from Haverah Park, Fly's Eye and HiRes at $E < 10^{20}$ eV, as well as of

⁶⁾The simplest example of this kind of a particle is a photon. We note that the current bounds on the photon content [34, 35] do not restrict the primaries at $E \gtrsim 10^{20}$ eV; to conclude about hadronic primaries from the shower profiles and muon counting in particular events, one needs much better statistics than available.

the AGASA events with zenith angles larger than 45° , would immediately enlarge the statistics without awaiting for the future experiments.

Finally, we comment on a recent proposal [8] that the discrepancy between the AGASA and HiRes fluxes at highest energies might be explained by different fields of view. Indeed, the HiRes' *differential* exposure peaks in the Northern region while one of AGASA has a maximum at $\delta \approx 36^\circ$, the AGASA detector's latitude. The "zone of avoidance" in the North affects the results of the flux measurements which usually assume the isotropic distribution of arrival directions. We estimate this effect by a rough assumption that the cosmic rays with $E \gtrsim 10^{20}$ eV are distributed uniformly at $\delta < 50^\circ$ but are absent at $\delta \geq 50^\circ$. With this assumption, a flux measured by HiRes would be about 40% smaller than one averaged over all sky, while a flux measured by AGASA decreases by about 20%. Clearly, this effect cannot eliminate the conflict between the two experiments.

The authors are indebted to S. Dubovsky, M. Fairbairn, O. Kalashev, V. Kuzmin, M. Libanov, V. Rubakov, D. Semikoz, M. Teshima, P. Tinyakov and I. Tkachev for numerous helpful discussions. This work was supported in part by RFBR grant 02-02-17398, by the grants of the President of the Russian Federation NS-2184.2003.2, MK-2788.2003.02 (D.G.), MK-1084.2003.02 (S.T.) and by the program SCOPES of the Swiss National Science Foundation, project No. 7SUPJ062239. The work of S.T. is supported in part by INTAS grant YSF 2001/2-129 and by a fellowship of the "Dynasty" foundation (awarded by the Scientific Council of ICFPM).

1. K. Greisen, Phys. Rev. Lett. **16** (1966) 748.
2. G. T. Zatsepin and V. A. Kuzmin, JETP Lett. **4** (1966) 78 [Pisma Zh. Eksp. Teor. Fiz. **4** (1966) 114].
3. N. Hayashida *et al.*, arXiv:astro-ph/0008102.
4. Y. Uchihori *et. al.*, Astropart. Phys. **13** (2000) 151.
5. P. G. Tinyakov and I. I. Tkachev, JETP Lett. **74** (2001) 1 [Pisma Zh. Eksp. Teor. Fiz. **74** (2001) 3].
6. M. Takeda *et. al.*, Proc. 19th Texas Symposium (Paris) 08/16 (1998).
7. W. Bednarek, New Astron. **7** (2002) 471.
8. T. Stanev, arXiv:astro-ph/0303123.
9. <http://www-akeno.icrr.u-tokyo.ac.jp/AGASA/results.html#100EeV>
10. P. Tinyakov and I. Tkachev, arXiv:hep-ph/0212223.
11. V. Berezinsky, A. Gazizov and S. Grigorjeva, arXiv:astro-ph/0302483.
12. P. G. Tinyakov and I. I. Tkachev, JETP Lett. **74**, 445 (2001) [Pisma Zh. Eksp. Teor. Fiz. **74**, 499 (2001)].
13. A. V. Uryson, Proc. 27th ICRC (Hamburg, 2001) 551.
14. D. S. Gorbunov *et al.*, Astrophys. J. **577** (2002) L93.
15. M. Kachelriess, D. V. Semikoz and M. A. Tortola, arXiv:hep-ph/0302161.
16. O. E. Kalashev, Ph.D. thesis (INR, Moscow, 2003).
17. X. Chi *et. al.*, J. Phys. G **18** (1992) 553.
18. M. Nagano and A. A. Watson, Rev. Mod. Phys. **72** (2000) 689.
19. M. Takeda *et al.*, arXiv:astro-ph/0209422.
20. T. Abu-Zayyad *et al.*, arXiv:astro-ph/0208243.
21. T. Abu-Zayyad *et al.*, arXiv:astro-ph/0208301.
22. Catalogue of Highest Energy Cosmic Rays, Vols. 1,2,3; World Data Center C2 for Cosmic Rays, Itabashi, Tokyo.
23. M. Ave *et al.*, Astropart. Phys. **19** (2003) 47.
24. M. A. Lawrence, R. J. Reid and A. A. Watson, J. Phys. G **17** (1991) 733.
25. <http://eas.ysn.ru/yakutsk.html>
26. D. J. Bird *et al.*, Astrophys. J. **441** (1995) 144.
27. J. A. Bellido, Ph.D. thesis (Univ. of Adelaide, 2002), http://www.cosmic-ray.org/thesis/bellido/thesis_jose.ps
28. Z. Cao, http://taws300.icrr.u-tokyo.ac.jp/workshop2003/viewgraph/Z_Cao.pdf
29. P. Sommers, Astropart. Phys. **14** (2001) 271.
30. N. W. Evans, F. Ferrer and S. Sarkar, Astropart. Phys. **17** (2002) 319.
31. J. Belz, *Anisotropy Studies of Ultra-High Energy Cosmic Rays as Observed by the High Resolution Fly's Eye (HiRes)*, presentation at the 27th ICRC, Hamburg, 2001.
32. W. Springer, <http://www.pi.infn.it/lathuile/2003/talks/Springer.pdf>
33. P. Sommers, http://anthrax.physics.indiana.edu/~teige/p_sommers.ps
34. M. Ave *et al.*, Phys. Rev. D **65** (2002) 063007.
35. K. Shinozaki *et al.*, Astrophys. J. **571** (2002) L117.